

Adsorption structure of macrocyclic energetic molecule DOATF on Au(111)

Xiao Chang(常霄), Li Huang(黄立), Yixuan Gao (高艺璇), Changjiang Yu(于长江), Yun Cao(曹云), Long Lv(吕龙), Xiao Lin(林晓), Shixuan Du(杜世萱), and Hong-Jun Gao(高鸿钧)

Citation: Chin. Phys. B, 2023, 32 (**9**): 096802. DOI: 10.1088/1674-1056/acda84

Journal homepage: http://cpb.iphy.ac.cn; http://iopscience.iop.org/cpb

What follows is a list of articles you may be interested in

Manipulating charge density wave state in kagome compound RbV_3Sb_5

Yu-Xin Meng(孟雨欣), Cheng-Long Xue(薛成龙), Li-Guo Dou(窦立国), Wei-Min Zhao(赵伟民), Qi-Wei Wang(汪琪玮), Yong-Jie Xu(徐永杰), Xiangqi Liu(刘祥麒), Wei Xia(夏威), Yanfeng Guo(郭艳峰), and Shao-Chun Li(李绍春)

Chin. Phys. B, 2023, 32 (**9**): 096801. DOI: 10.1088/1674-1056/acd8b1

Selective formation of ultrathin PbSe on Ag(111)

Jing Wang(王静), Meysam Bagheri Tagani, Li Zhang(张力), Yu Xia(夏雨), Qilong Wu(吴奇龙), Bo Li(黎博), Qiwei Tian(田麒玮), Yuan Tian(田园), Long-Jing Yin(殷隆晶), Lijie Zhang(张利杰), and Zhihui Qin(秦志辉)

Chin. Phys. B, 2022, 31 (**9**): 096801. DOI: 10.1088/1674-1056/ac7867

Phase transition-induced superstructures of *β*-Sn films with atomic-scale thickness

Le Lei(雷乐), Feiyue Cao(曹飞跃), Shuya Xing(邢淑雅), Haoyu Dong(董皓宇), Jianfeng Guo(郭剑锋), Shangzhi Gu(顾尚志), Yanyan Geng(耿燕燕), Shuo Mi(米烁), Hanxiang Wu(吴翰翔), Fei Pang(庞斐), Rui Xu(许瑞), Wei Ji(季威), and Zhihai Cheng(程志海)

Chin. Phys. B, 2021, 30 (**9**): 096804. DOI: 10.1088/1674-1056/ac11e8

Epitaxial growth of antimony nanofilms on HOPG and thermal desorption to control the film thickness

Shuya Xing(邢淑雅), Le Lei(雷乐), Haoyu Dong(董皓宇), Jianfeng Guo(郭剑峰), Feiyue Cao(曹飞跃), Shangzhi Gu(顾尚志), Sabir Hussain, Fei Pang(庞斐), Wei Ji(季威), Rui Xu(许瑞), Zhihai Cheng(程志海)

Chin. Phys. B, 2020, 29 (**9**): 096801. DOI: 10.1088/1674-1056/aba27c

STM study of selenium adsorption on Au(111) surface

Bin Liu(刘斌), Yuan Zhuang(庄源), Yande Que(阙炎德), Chaoqiang Xu(徐超强), Xudong Xiao(肖旭东)

Chin. Phys. B, 2020, 29 (**5**): 056801. DOI: 10.1088/1674-1056/ab821d

---

Adsorption structure of macrocyclic energetic molecule DOATF on Au(111)

Xiao Chang(常霄)[1], Li Huang(黄立)[1,†], Yixuan Gao(高艺璇)[1], Changjiang Yu(于长江)[2], Yun Cao(曹云)[1], Long Lv(吕龙)[2], Xiao Lin(林晓)[1], Shixuan Du(杜世萱)[1], and Hong-Jun Gao(高鸿钧)[1]

[1] *Institute of Physics & University of Chinese Academy of Sciences, Chinese Academy of Sciences, Beijing* 100190, *China*
[2] *Shanghai Institute of Organic Chemistry, Chinese Academy of Sciences, Shanghai* 200032, *China*

(Received 1 March 2023; revised manuscript received 26 May 2023; accepted manuscript online 1 June 2023)

Furazan macrocyclic compound 3,4:7,8:11,12:15,16-tetrafurazan-1,9-dioxazo-5,13- diazocyclohexadecane (DOATF) is an ideal energetic material with high heat of formation. Here, using scanning tunneling microscopy (STM) and non-contact atomic force microscopy (nc-AFM), we investigated the adsorption structure of DOATF molecules on Au(111) surface, which shows the four furanzan rings in the STM images and a bright protrusion off the center of the molecule in the nc-AFM images. Combined with density functional theory (DFT) calculations, we confirmed that the bright feature in the nc-AFM images is an N–O coordinate bond pointing upwards in one of the two azoxy groups; while the other N–O bond pointing towards the Au(111) surface. Our work contributes for a deeper understanding of the adsorption structure of macrocyclic compounds, which would promote the designing of DOATF-metal frameworks.

Keywords: STM, nc-AFM, DFT calculations, furazan macrocylic compound, energetic material

PACS: 68.37.Ps, 71.15.Mb, 07.79.Cz **DOI:** 10.1088/1674-1056/acda84

1. Introduction

Furazan macrocyclic compounds, exhibiting excellent energetic performance and good molecular stability, have great potential in applications, such as propellants, explosives and pyrotechnics.[1–9] 3,4:7,8:11,12:15,16-tetrafurazan-1,9-dioxazo-5,13-diazocyclohexadecane (DOATF), a furazan-based heterocyclic molecule, has been demonstrated to have a superior standard enthalpy of formation than most energetic materials since its first synthesis in 1996.[1,10] Meanwhile, DOATF has large detonation velocity, suggesting it as an ideal propellant. Combined with the new concept of using metal–organic frameworks (MOFs) as high explosives,[11] MOF with furazan ligands have been synthesized and demonstrated as high-energy density materials.[12] However, MOFs with furazan macrocyclic molecules, such as DOATF, have yet to be further investigated, of which the interaction between metal atoms and furazan macrocyclic molecules is of vital importance.

Scanning tunneling microscopy (STM) and non-contact atomic force microscopy (nc-AFM) are powerful surface investigation methods to image the sample down to atomic- and chemical-bond-resolution in real-space.[13] Using STM and nc-AFM, the adsorption structures of organic molecules on metal surfaces can be clearly resolved,[14,15] which gives us information on the interaction between the molecule and the metal atoms.[16–19] In this regard, studying the adsorption structure of DOATF can contribute for rational design of DOATF-based energetic MOFs.

Here, we investigated the adsorption structure of DOATF on Au(111) surface by STM, nc-AFM, and density functional theory (DFT) simulations. The STM images show that DOATF has a planar adsorption structure in quatrefoil shape, which can be attributed to the four furazan groups in the macrocycle plane. Nc-AFM images reveal that there is an out-of-plane atom on top of the macrocycle plane, sitting off the center of the macrocycle. Combined with DFT simulations, this out-of-plane atom is confirmed to be the oxygen atom in the coordinate N–O bonds in one of the azoxy groups.

2. Methods

2.1. Sample preparation, STM/AFM measurement

The experiments were performed using a CreaTec ultra-high vacuum (UHV) low-temperature STM/nc-AFM system with a base pressure of 2×10^{-10} mbar (1 bar = 10^5 Pa). The Au(111) surface was cleaned by repeated cycles of Ar^+ ion sputtering and subsequent annealing at 700 K for 20 min. The DOATF were sublimated at 350 K onto the Au(111) substrate, which was held at room temperature during molecular deposition. All STM and nc-AFM measurements were performed at 5 K with a qPlus sensor.[20] STM topography images were acquired in constant current mode and the voltages represented the bias on the sample with respect to the tip. Nc-AFM images were obtained in the frequency modulation mode using a CO-functionalized tip.[21]

†Corresponding author. E-mail: lhuang@iphy.ac.cn

© 2023 Chinese Physical Society and IOP Publishing Ltd

2.2. First-principles calculations

All DFT calculations are carried out using Vienna *ab initio* simulation package (VASP) with the projector augmented wave (PAW) method, and a generalized gradient approximation (GGA) in the form of Perdew–Burke–Ernzerhof (PBE) is adopted for the exchange–correlation functional.[22–24] The energy cutoff of the plane-wave basis sets is 400 eV. Long-range dispersion corrections have been taken into account within a DFT-D2 approach of Grimme.[25] In all calculations, the Au(111) substrate was modeled by three-layered slabs where the bottom one layer was fixed. The atomic structures were relaxed until the residual forces on all unconstrained atoms were less than 0.01 eV/Å. AFM simulation images were obtained by the DFT optimized geometries. The probe particle model is used in the AFM simulation based on classical force-fields.[26]

3. Results and discussion

The chemical structure of DOATF molecule is shown in Fig. 1(a), which has four furazan rings (blue dashed boxes) connected into a macrocycle by two azo groups (orange dashed boxes) and two azoxy groups (red dashed boxes). The azo (azoxy) groups sit at the opposite sides of the macrocycle. The azoxy group have an additional N–O coordinate bond compared with the azo group, indicating that they should have different contrast in the STM images.

The DOATF molecules were sublimed from a molecule cell evaporator at 350 K onto a clean Au(111) substrate held at 80 K in ultrahigh vacuum. Figure 1(b) shows the large-scale topographic image of as-deposited DOATF on Au(111), in which most DOATF molecules gather into small assemblies on the terraces and at the step edges of the substrate. The DOATF molecules have a square shape with four lobes, as indicated in Fig. 1(c) by the four blue dashed boxes, of which two side-by-side lobes are brighter than the other two. One side of the square shaped DOATF molecules is along the $[11\bar{2}]$ or $[1\bar{1}0]$ direction of the substrate. According to the structural symmetry, the four lobes are most likely to be the furazan groups, not the diagonally distributed azo or azoxy groups.

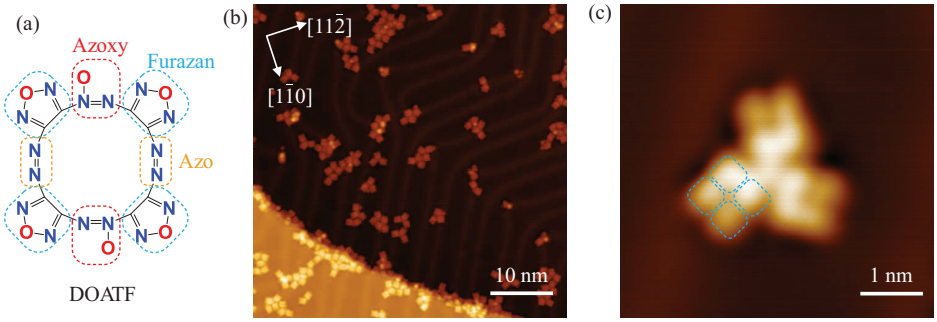


Fig. 1. STM images of DOATF molecules adsorbed on Au(111) surface. (a) Chemical structure of DOATF. The azoxy, furazan, and azo groups are labelled by red, blue, and orange dashed boxes, respectively. (b) Large-scale STM image of DOATF molecules as deposited on Au(111) surface ($V_s = -300$ mV, $I_t = 30$ pA). (c) Zoom-in STM image of a DOATF trimer ($V_s = -200$ mV, $I_t = 20$ pA). The four blue dashed boxes superposed on one of the molecules denote the four-petal morphology of a DOATF monomer on Au(111).

To understand why the four identical furazan groups have two contrasts in the STM images, we carried out nc-AFM measurements on a DOATF trimer in the same area as shown in Fig. 2(a). Figures 2(b)–2(d) display a sequence of constant-height nc-AFM images with decreasing tip-sample distances. When the tip is relative far from the molecules (Fig. 2(b)), the four furazan rings have vague shapes in dark contrast due to the reason that they are still in the attraction force region (denoted by the four bule dashed boxes). Meanwhile, a prominent bright protrusion is imaged off the center of each molecule (red dashed circles), which is a clear feature caused by repulsive forces, indicating there is an out-of-plane atom on top of the macrocycle plane. Compared with the STM image in Fig. 2(a), the two lobes beneath the bright protrusion have darker contrast than the other two lobes in each molecule, indicating the out-of-plane atom has lower density of states than the furazan rings.

With decreasing tip-sample distance in Fig. 2(c), the signal from repulsive force starts to emerge from the dark hollows at the position of the furazan rings (bule dashed boxes) and on two sides of the molecule (orange dashed circles). The latter features may correspond to the N=N bonds in azo or azoxy groups, which needs to be confirmed by images with more details. By further approaching the tip to the sample, clear repulsive feature of bond-resolution furazan rings are obtained in Fig. 2(d) (blue dashed boxes). There are also bright line-features connecting the out-of-plane atom with the N=N bonds and part of the furazan rings. Another important feature is a bond extending from the opposite position of the out-of-plane atom, which, judging from the contrast, is a bond that slantingly points to the underneath Au(111) surface (green dashed rectangle). Since the only possible out-of-plane bonds in DOATF are the N–O coordinate bonds in azoxy groups, the positions marked by the red dashed circle and the green

dashed rectangle corresponds to the azoxy groups. Consequently, the positions where the orange dashed circles marked are azo groups.

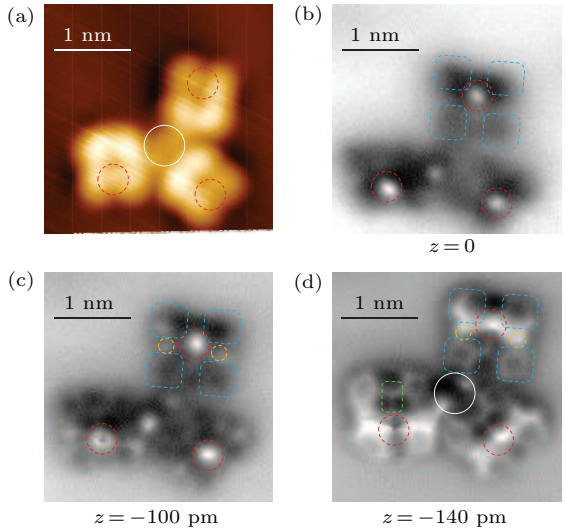


Fig. 2. Chemical-bond-resolved nc-AFM images of a DOATF trimer at different scanning heights. (a) STM image of a DOATF trimer ($V_s = -200$ mV, $I_t = 10$ pA). (b)–(d) nc-AFM images of the same DOATF trimer in panel (a) at decreasing scanning heights of 0 pm, −100 pm, and −140 pm relative to a tunneling point of $V_s = -200$ mV and $I_t = 10$ pA. The scanning oscillation amplitude was 100 pm. The blue dashed boxes denote the furazan groups; the red dashed circles marked an atom that is higher than the macrocycle plane, which can be attributed to an oxygen atom in one of the azoxy groups; the orange dashed circles indicate the azo groups; the white solid circles indicate the gold adatoms between the DOATF monomers.

In Fig. 2(a), the area between the DOATF monomers appears higher than the substrate, as denoted by a solid-line circle. In the corresponding nc-AFM image in Fig. 2(d), there are two bright spots in this area, with bright line features extending to the furazan groups, which indicates there are gold adatoms interacting with the furazan groups in the DOATF assemblies. Since the reconstructed Au(111) surface has plenty of gold adatoms itself, and the N atoms have a stronger interaction with gold compared to the C skeleton, the rich N dopants in DOATF monomers are the most possible reason for the formation of such DOATF-adatom assemblies.

To further verify the above discussions, we performed nc-AFM simulations based on DFT calculations. Figure 3(a) is the optimized structure of DOATF adsorbed on Au(111) surface, in which the macrocyclic ring is nearly planar. One of the N–O coordinate bond points upward from the macrocyclic plane (marked by the red dashed circle), while the other N–O coordinate bond points downward to the substrate, as shown in the side view. Since the N (O) atoms are negatively (positively) charged in the coordinate bonds, this structure indicates that the two N–O coordinate bonds act as a pair of dipoles on the upper and lower surface of the macrocycle of DOATF. Figures 3(b)–3(d) display the zoomed-in nc-AFM images of the molecule in the upper right part in Fig. 2 with decreasing tip-sample distances. The corresponding DFT simulated images are shown in Figs. 3(e)–3(g). Both experimental and simulated images show a prominent bright protrusion at a relatively far-away scanning distance, which is the oxygen atom above the macrocyclic plane, as marked by the red dashed circle in each image. At close scanning distance, the simulated image nearly mimics the experimental image, clearing displays the four furazan rings, the azo groups, and the vague N–O bond that underneath the macrocyclic plane.

Since the DOATF monomers form assemblies with gold adatoms, the nc-AFM images in Figs. 3(b)–3(d) were taken on a DOATF monomer in a trimer. The presence of the adatoms mainly influences the interactions with the furazan groups. Therefore, in the nc-AFM images, the macrocycle looks flatter than the monomer without adatoms in the DFT simulated images. However, for the N–O bond that does not have direct interaction with the gold adatoms, the experimental feature and the DFT simulation have good consistence.

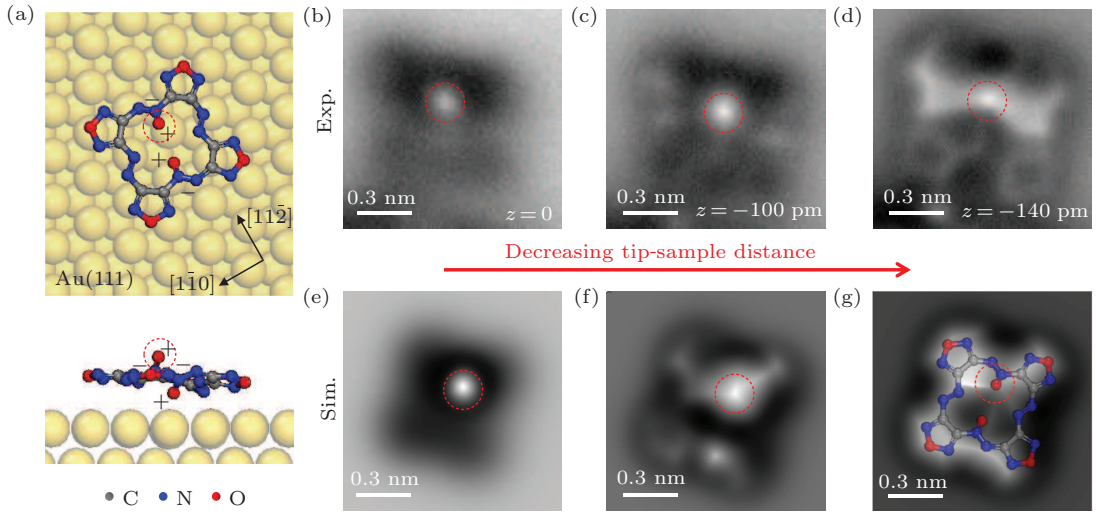


Fig. 3. DFT simulations and nc-AFM images of a DOATF monomer adsorbed on Au(111) surface. (a) DFT optimized adsorption structure of a DOATF monomer on Au(111) surface. (b)–(d) nc-AFM images of a DOATF monomer on Au(111) at decreasing tip-sample distances of 0 pm, −100 pm, and −140 pm relative to a tunneling point of $V_s = -200$ mV and $I_t = 10$ pA. The oscillation amplitude was 100 pm. (e)–(g) The DFT simulated nc-AFM images at decreasing tip-sample distance. The chemical structure of DOATF is superposed in panel (g).

4. Conclusion

We resolved the adsorption structure of DOATF molecules on Au(111) substrate by STM and nc-AFM scanning. In STM images, the DOATF has a four-lobed square shape, which correspond to the four furazan group as revealed by nc-AFM images. The nc-AFM images show a bright protrusion off the center of the molecule, indicating a non-planar structure. Combined with DFT calculations, we confirm that the macrocycle consisted of four furazan groups, two azo groups, and two azoxy groups is nearly planar when DOATF adsorbs on Au(111), with the two N–O coordinate bonds pointing upwards and downwards from the macrocyclic plane. Our work clearly unveiled the adsorption structure of macrocyclic energy material DOATF on Au(111), which may contribute to deeper understanding of the interactions between DOATF and metal atoms in designing of DOATF-based metal–organic frameworks.

Acknowledgements

Project supported by the National Key Research and Development Projects of China (Grant No. 2019YFA0308500), the National Natural Science Foundation of China (Grant No. 61888102), and the Funds from the Chinese Academy of Sciences (Grant Nos. XDB30000000 and YSBR-003).

References

[1] Sheremetev A B, Kulagina V O and Ivanova E A 1996 *J. Organ. Chem.* **61** 1510
[2] Sheremetev A B, Kharitonova O V, Mel'nikova T y M, Novikova T y S, Kuz'min V S and Khmel'nitskii L I 1996 *Mendeleev Commun.* **6** 141
[3] Sheremetev A B, Mantseva E V, Dmitriev D E and Sirovskii F S 2002 *Russ. Chem. B* **51** 659
[4] Suponitsky K Y, Lyssenko K A, Ananyev I V, Kozeev A M and Sheremetev A B 2014 *Cryst. Growth Des.* **14** 4439
[5] Veauthier J M, Chavez D E, Tappan B C and Parrish D A 2010 *Journal of Energetic Materials* **28** 229
[6] Wang X, Xu K, Sun Q, Wang B, Zhou C and Zhao F 2015 *Propellants, Explosives, Pyrotechnics* **40** 9
[7] Sheremetev A B, Makhova N N and Friedrichsen W 2001 *Advances in Heterocyclic Chemistry*, Vol. **78**, p. 65 (San Diego: Academic Press)
[8] Suntsova M A and Dorofeeva O V 2017 *Journal of Molecular Graphics and Modelling* **72** 220
[9] Zhang J, Zhou J, Bi F and Wang B 2020 *Chin. Chem. Lett.* **31** 2375
[10] Xiaohong L, Ruizhou Z and Xianzhou Z 2013 *Struct. Chem.* **24** 1193
[11] Zhang Q and Shreeve J N M 2014 *Angewandte Chemie-International Edition* **53** 2540
[12] Gong L, Chen G, Liu Y, Wang T, Zhang J, Yi X and He P 2021 *New Journal of Chemistry* **45** 22299
[13] Gross L, Mohn F, Moll N, Liljeroth P and Meyer G 2009 *Science* **325** 1110
[14] Rizzo D J, Veber G, Cao T, Bronner C, Chen T, Zhao F, Rodriguez H, Louie S G, Crommie M F and Fischer F R 2018 *Nature* **560** 204
[15] Ruffieux P, Wang S, Yang B, Sánchez-Sánchez C, Liu J, Dienel T, Talirz L, Shinde P, Pignedoli C A, Passerone D, Dumslaff T, Feng X, Müllen K and Fasel R 2016 *Nature* **531** 489
[16] Mieres-Perez J, Lucht K, Trosien I, Sander W, Sanchez-Garcia E and Morgenstern K 2021 *J. Am. Chem. Soc.* **143** 4653
[17] Jiang L, Zhang B, Medard G, Seitsonen A P, Haag F, Allegretti F, Reichert J, Kuster B, Barth J V and Papageorgiou A C 2017 *Chem. Sci.* **8** 8301
[18] Bakker A, Freitag M, Kolodzeiski E, Bellotti P, Timmer A, Ren J, Schulze Lammers B, Moock D, Roesky H W, Monig H, Amirjalayer S, Fuchs H and Glorius F 2020 *Angew. Chem. Int. Ed. Engl.* **59** 13643
[19] Qi J, Gao Y X, Huang L, Lin X, Dong J J, Du S X and Gao H J 2019 *Chin. Phys. B* **28** 066801
[20] Giessibl F J 2019 *Rev. Sci. Instrum.* **90** 011101
[21] Bartels L, Meyer G and Rieder K H 1997 *Appl. Phys. Lett.* **71** 213
[22] Kresse G and Furthmuller J 1996 *Comp. Mater. Sci.* **6** 15
[23] Kresse G and Furthmuller J 1996 *Phys. Rev. B* **54** 11169
[24] Perdew J P, Burke K and Ernzerhof M 1996 *Phys. Rev. Lett.* **77** 3865
[25] Grimme S 2006 *J. Comput. Chem.* **27** 1787
[26] Hapala P, Kichin G, Wagner C, Tautz F S, Temirov R and Jelinek P 2014 *Phys. Rev. B* **90** 085421